differences in intensity between Friedel opposites, *hkl* and $\overline{hkl}$, are hidden in a powder-diffraction pattern and the techniques of Section 1.6.5.1 are inapplicable. It is also known that experimental results on structure-factor statistics described in Section 1.6.2.2 are sensitive to the algorithm used to extract the integrated Bragg intensities from the powder-diffraction pattern. One procedure tends to produce intensity statistics typical of the noncentrosymmetric space group $P1$ and another those of the centrosymmetric space group $P\overline{1}$. In all, nothing much can be learnt from stage 2 for a powder-diffraction pattern. As a consequence, space-group determination from powder diffraction relies entirely on the Bravais lattice derived from the indexing of the diffraction pattern in stage 1 and the detection of systematic absences in stage 3.

(3) Stage 3 concerns the identification of the conditions for possible systematic absences. However, Bragg-peak overlap causes difficulties with determining systematic absences. For powder-diffraction peaks at small values of $\sin\theta/\lambda$, the problem is rarely severe, even for low-resolution laboratory powder-diffraction data. Potentially absent reflections at higher values of $\sin\theta/\lambda$ often overlap with other reflections of observable intensity. Accordingly, conclusions about the presence of space-group symmetry operations are generally drawn on the basis of a very small number of clear intensity observations. Observing lattice-centring absences is usually relatively easy. In the case of molecular organic materials, considerable help in space-group selection comes from the well known frequency distribution of space groups, where some 80% of compounds crystallize in one of the following: $P2_1/c$, $P\overline{1}$, $P2_12_12_1$, $P2_1$ and $C2/c$. Practical methods of proceeding are described by David & Sivia (2002). It should also be pointed out that Table 1.6.4.1 in this chapter may often be found to be helpful. For example, if it is known that the Bravais lattice is of type *cP*, Table 1.6.4.1 tells us that the possible Laue classes are $m\overline{3}$ and $m\overline{3}m$ and the possible space groups can be found in Tables 1.6.4.25 and 1.6.4.26, respectively. The appropriate reflection conditions are of course given in these tables. All relevant tables can thus be located with the aid of Table 1.6.4.1 if the Bravais lattice is known.

There has been considerable progress since 2000 in the automated extraction by software of the set of conditions for reflections from a powder-diffraction pattern for undertaking stage 3 above. Once the conditions have been identified, Tables 1.6.4.2–1.6.4.30 are used to identify the corresponding space groups. The output of such software consists of a ranked list of complete sets of conditions for reflections (*i.e.* the horizontal rows of conditions given in Tables 1.6.4.2–1.6.4.30). Accordingly, the best-ranked set of conditions is at the top of the list followed by others in decreasing order of appropriateness. The list thus is answering the question: Which is the most probable set of reflection conditions for the data to hand? Such software uses integrated intensities of Bragg reflections extracted from the powder pattern and, as mentioned above, the results are sensitive to the particular profile integration procedure used. Moreover, only ideal Wilson (1949) p.d.f.'s for space groups $P1$ and $P\overline{1}$ are implemented. The art of such techniques is to find appropriate criteria such that the most likely set of reflection conditions is clearly discriminated from any others. Altomare *et al.* (Altomare, Caliandro, Camalli, Cuocci, da Silva *et al.*, 2004; Altomare, Caliandro, Camalli, Cuocci, Giacovazzo *et al.*, 2004; Altomare *et al.*, 2005, 2007, 2009) have used a probabilistic approach combining the probabilities of individual symmetry operations of candidate space groups. The approach is pragmatic and has evolved over several versions of the software. Experience has accumulated through use of the procedure and the discrimination of the software has consequently improved. Markvardsen *et al.* (2001, 2012) commence with an in-depth probabilistic analysis using the concepts of Bayesian statistics which was demonstrated on a few test structures. Later, Markvardsen *et al.* (2008) made software generally available for their approach. Vallcorba *et al.* (2012) have also produced software for space-group determination, but give little information on their algorithm.

1.6.6. Space groups for nanocrystals by electron microscopy

By J. C. H. Spence

The determination of crystal space groups may be achieved by the method of convergent-beam electron microdiffraction (CBED) using a modern transmission electron microscope (TEM). A detailed description of the CBED technique is given by Tanaka (2008) in Section 2.5.3 of Volume B; here we give a brief overview of the capabilities of the method for space-group determination, for completeness. A TEM beam focused to nanometre dimensions allows study of nanocrystals, while identification of noncentrosymmetric crystals is straightforward, as a result of the strong multiple scattering normally present in electron diffraction. (Unlike single scattering, this does not impose inversion symmetry on diffraction patterns, but preserves the symmetry of the sample and its boundaries.) CBED patterns also allow direct determination of screw and glide space-group elements, which produce characteristic absences, despite the presence of multiple scattering, in certain orientations. These absences, which remain for all sample thicknesses and beam energies, may be shown to occur as a result of an elegant cancellation theorem along symmetry-related multiple-scattering paths (Gjønnes & Moodie, 1965). Using all of the above information, most of the 230 space groups can be distinguished by CBED. The remaining more difficult cases (such as space groups that differ only in the location of their symmetry elements) are discussed in Spence & Lynch (1982), Eades (1988), and Saitoh *et al.* (2001). Enantiomorphic pairs require detailed atomistic simulations based on a model, as in the case of quartz (Goodman & Secomb, 1977). Multiple scattering renders Bragg intensities sensitive to structure-factor phases in noncentrosymmetric structures, allowing these to be measured with a tenth of a degree accuracy (Zuo *et al.*, 1993). Unlike X-ray diffraction, electron diffraction is very sensitive to ionicity and bonding effects, especially at low angles, allowing extinction-free charge-density mapping with high accuracy (Zuo, 2004; Zuo *et al.*, 1999). Because of its sensitivity to strain, CBED may also be used to map out local phase transformations which cause space-group changes on the nanoscale (Zuo, 1993; Zhang *et al.*, 2006).

In simplest terms, a CBED pattern is formed by enlarging the incident beam divergence in the transmission diffraction geometry, as first demonstrated G. Mollenstedt in 1937 (Kossel & Mollenstedt, 1942). Bragg spots are then enlarged into discs, and the intensity variation within these discs is studied, in addition to that of the entire pattern, in the CBED method. The intensity variation within a disc displays a complete rocking curve in each of the many diffracted orders, which are simultaneously excited

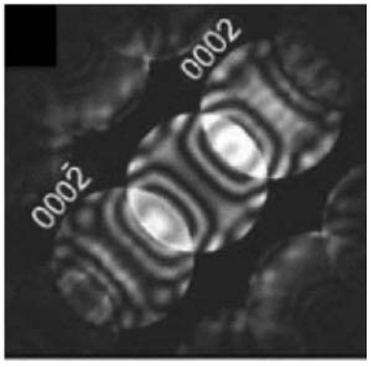

Figure 1.6.6.1
Polarity determination by convergent-beam electron diffraction. A CBED pattern from ZnO with the beam normal to the *c* axis is shown. The intensity distribution along **c** does not have inversion symmetry, reflecting the noncentrocentrosymmetric nature of the structure. Reproduced with permission from Wang *et al.* (2003). Copyright (2003) by The American Physical Society.

and recorded. The entire pattern thus consists of many independent 'point' diffraction patterns (each for a slightly different incident beam direction) laid beside each other. Fig. 1.6.6.1 shows a CBED pattern from the wurtzite structure of ZnO, with the beam normal to the *c* axis (Wang *et al.*, 2003). The intensity variation along a line running through the centres of these discs (along the *c* axis) is not an even function, strongly violating Friedel's law for this elastic scattering. At higher scattering angles, curvature of the Ewald sphere allows three-dimensional symmetry elements to be determinated by taking account of 'out-of-zone' intensities in the outer higher-order Laue zone (HOLZ) rings near the edge of the detector. Since sub-ångstrom-diameter electron probes and nanometre X-ray laser probes (Spence *et al.*, 2012) are now being used, the effect of the inevitable coherent interference between overlapping convergent-beam orders on space-group determination must be considered (Spence & Zuo, 1992).

A systematic approach to space-group determination by CBED has been developed by several groups. In general, one would determine the symmetry of the projection diffraction group first (ignoring diffraction components along the beam direction z), then add the z-dependent information seen in HOLZ lines, allowing one to finally identify the point group from tables, by combining all this information. After indexing the pattern, in order to determine a unit cell the Bravais lattice is next determined. The form of the three-dimensional reciprocal lattice and its centring can usually be determined by noting the registry of Bragg spots in a HOLZ ring against those in the zero-order (ZOLZ) ring. Finally, by setting up certain special orientations, tests are applied for the presence of screw and glide elements, which are revealed by a characteristic dark line or cross within the CBED discs. Tables can again then be used to combine these translational symmetry elements with the previously determined point group, to find the space group. As a general experimental strategy, one first seeks mirror lines (perhaps seen in Kikuchi patterns), then follows these around using the two-axis goniometer fitted to modern TEM instruments in a systematic search for other symmetry elements. Reviews of the CBED method can be found in Steeds & Vincent (1983), in Goodman (1975), and in the texts by Tanaka *et al.* (1988). A textbook-level worked example of space-group determination by CBED can be found in Spence & Zuo (1992) and in the chapter by A. Eades in Williams & Carter (2009).

References

Allenmark, S., Gawronski, J. & Berova, N. (2007). Editors. *Chirality*, **20**, 605–759.

Altomare, A., Caliandro, R., Camalli, M., Cuocci, C., da Silva, I., Giacovazzo, C., Moliterni, A. G. G. & Spagna, R. (2004). *Space-group determination from powder diffraction data: a probabilistic approach*. *J. Appl. Cryst.* **37**, 957–966.

Altomare, A., Caliandro, R., Camalli, M., Cuocci, C., Giacovazzo, C., Moliterni, A. G. G. & Rizzi, R. (2004). *Automatic structure determination from powder data with EXPO2004*. *J. Appl. Cryst.* **37**, 1025–1028.

Altomare, A., Camalli, M., Cuocci, C., da Silva, I., Giacovazzo, C., Moliterni, A. G. G. & Rizzi, R. (2005). *Space group determination: improvements in EXPO2004*. *J. Appl. Cryst.* **38**, 760–767.

Altomare, A., Camalli, M., Cuocci, C., Giacovazzo, C., Moliterni, A. G. G. & Rizzi, R. (2007). *Advances in space-group determination from powder diffraction data*. *J. Appl. Cryst.* **40**, 743–748.

Altomare, A., Camalli, M., Cuocci, C., Giacovazzo, C., Moliterni, A. & Rizzi, R. (2009). *EXPO2009: structure solution by powder data in direct and reciprocal space*. *J. Appl. Cryst.* **42**, 1197–1202.

Authier, A., Borovik-Romanov, A. S., Boulanger, B., Cox, K. G., Dmitrienko, V. E., Ephraïm, M., Glazer, A. M., Grimmer, H., Janner, A., Jannsen, T., Kenzelmann, M., Kirfel, A., Kuhs, W. F., Küppers, H., Mahan, G. D., Ovchinnikova, E. N., Thiers, A., Zarembowitch, A. & Zyss, J. (2014). *International Tables for Crystallography*, Volume D, *Physical Properties of Crystals*, edited by A. Authier, 2nd edition, Part 1. Chichester: Wiley.

Boček, P., Hahn, Th., Janovec, V., Klapper, H., Kopský, V., Přivratska, J., Scott, J. F. & Tolédano, J.-C. (2014). *International Tables for Crystallography*, Volume D, *Physical Properties of Crystals*, edited by A. Authier, 2nd ed., Part 3. Chichester: Wiley.

Buerger, M. J. (1935). *The application of plane groups to the interpretation of Weissenberg photographs*. *Z. Kristallogr.* **91**, 255–289.

Buerger, M. J. (1942). *X-ray Crystallography*, ch. 22. New York: Wiley.

Buerger, M. J. (1946). *The interpretation of Harker syntheses*. *J. Appl. Phys.* **17**, 579–595.

Buerger, M. J. (1969). *Diffraction symbols*. In *Physics of the Solid State*, edited by S. Balakrishna, ch. 3, pp. 27–42. London: Academic Press.

Burzlaff, H., Zimmermann, H. & de Wolff, P. M. (2002). *Crystal lattices*. In *International Tables for Crystallography*, Volume A, *Space-Group Symmetry*, edited by Th. Hahn, 5th ed., Part 9. Dordrecht: Kluwer Academic Publishers.

David, W. I. F. & Shankland, K. (2008). *Structure determination from powder diffraction data*. *Acta Cryst.* A**64**, 52–64.

David, W. I. F., Shankland, K., McCusker, L. B. & Baerlocher, Ch. (2002). Editors. *Structure Determination from Powder Diffraction Data*. IUCr Monograph No. 13. Oxford University Press.

David, W. I. F. & Sivia, D. S. (2002). *Extracting integrated intensities from powder diffraction patterns*. In *Structure Determination from Powder Diffraction Data*, edited by W. I. F. David, K. Shankland, L. B. McCusker & Ch. Baerlocher. IUCr Monograph No. 13. Oxford University Press.

Eades, J. A. (1988). *Glide planes and screw axes in CBED*. In *Microbeam Analysis 1988*, edited by D. Newberry, pp. 75–78. San Francisco Press.

Evans, P. (2006). *Scaling and assessment of data quality*. *Acta Cryst.* D**62**, 72–82.

Evans, P. R. (2011). *An introduction to data reduction: space-group determination, scaling and intensity statistics*. *Acta Cryst.* D**67**, 282–292.

Flack, H. D. (2003). *Chiral and achiral crystal structures*. *Helv. Chim. Acta*, **86**, 905–921.

Flack, H. D. (2015). *Methods of space-group determination – a supplement dealing with twinned crystals and metric specialization*. *Acta Cryst.* C**71**, 916–920.

Flack, H. D., Sadki, M., Thompson, A. L. & Watkin, D. J. (2011). *Practical applications of averages and differences of Friedel opposites*. *Acta Cryst.* A**67**, 21–34.

Flack, H. D. & Shmueli, U. (2007). *The mean-square Friedel intensity difference in P1 with a centrosymmetric substructure*. *Acta Cryst.* A**63**, 257–265.

Giacovazzo, C. (2008). *Direct methods*. In *International Tables for Crystallography*, Volume B, *Reciprocal Space*, edited by U. Shmueli, ch. 2.2, pp. 215–243. Dordrecht: Springer.

Gjønnes, J. & Moodie, A. F. (1965). *Extinction conditions in the dynamic theory of electron diffraction*. *Acta Cryst.* **19**, 65–69.